Available online at www.sciencedirect.com
SCIENCE DIRECT®
Journal of Power Sources 129 (2004) 38–44
JOURNAL OF POWER SOURCES
www.elsevier.com/locate/jpowsour

Nanostructured electrodes for next generation rechargeable electrochemical devices

A. Singhal [a,*], G. Skandan [a], G. Amatucci [b], F. Badway [b], N. Ye [c], A. Manthiram [c], H. Ye [d], J.J. Xu [d]

[a] *NEI Corporation, Piscataway, NJ 08854, USA*
[b] *Energy Storage Research Group, Rutgers University, Piscataway, NJ 08854, USA*
[c] *Department of Materials Science and Engineering, University of Texas, Austin, TX, USA*
[d] *Department of Ceramic and Materials Engineering, Rutgers University, Piscataway, NJ 08854, USA*

Abstract

Nanostructured intercalating electrodes offer immense potential for significantly enhancing the performance of rechargeable rocking chair (e.g. Li^+ and Mg^{2+}) and asymmetric hybrid batteries. The objective of this work has been to develop a variety of cathode (e.g. V_2O_5, $LiMnO_2$ and $LiFePO_4$) and anode (e.g. $Li_4Ti_5O_{12}$) materials with unique particle characteristics and controlled composition to reap the maximum benefits of nanophase electrodes for rechargeable Li-based batteries. Different processing routes, which were chosen on the basis of the final composition and the desired particle characteristics of electrode materials, were developed to synthesize a variety of electrode materials. Vapor phase processes were used to synthesize nanopowders of V_2O_5 and TiO_2. TiO_2 was the precursor used for producing ultrafine particles of $Li_4Ti_5O_{12}$. Liquid phase processes were used to synthesize nanostructured $LiMn_xM_{1-x}O_2$ and $LiFePO_4$ powders. It was found that (i) nanostructured V_2O_5 powders with a metastable structure have 30% higher retention capacity than their coarse-grained counterparts, for the same number of cycles; (ii) the specific capacity of nanostructured $LiFePO_4$ cathodes can be significantly improved by intimately mixing nanoparticles with carbon particles and that cathodes made of $LiFePO_4$/C composite powder exhibited a specific capacity of ∼145 mAh/g (85% of the theoretical capacity); (iii) nanostructured, layered $LiMn_xM_{1-x}O_2$ cathodes demonstrated a discharge capacity of ∼245 mAh/g (86% of the theoretical capacity) at a slow discharge rate; however, the composition and structure of nanoparticles need to be optimized to improve their rate capabilities and (iv) unlike micron-sized (1–10 μm) powders, ultrafine $Li_4Ti_5O_{12}$ showed exceptional retention capacity at a discharge rate as high as 10 C in Li-test cells.

Keywords: Nanostructured electrode; Li-based batteries; Asymmetric hybrid devices; High energy density; Fast rate capabilities; Cathode

1. Introduction

Of all the rechargeable batteries, the Li-ion battery is becoming the system of choice to power many portable and non-portable devices because of its light weight, good overall performance and high energy density, 125–150 Wh/kg [1]. Compared to other battery technologies, such as lead acid, nickel–cadmium and nickel–metal hydride batteries, rechargeable rocking chair batteries, including Li-ion and Mg-ion batteries, are still immature and there is a room for significant improvement. As suggested in a recent review, improvements in the performance of Li-based energy storage devices should arise from changes in cell chemistry and engineering [2].

Areas where improvements are needed concern the energy density, the rate capability and cost of batteries. State-of-the-art Li-ion batteries use coarse-grained electrode materials: carbon as an anode and $LiCoO_2$ as a cathode material. $LiCoO_2$ has a practical energy density of ∼500 Wh/kg. There have been significant efforts to improve the energy density of cathode materials either by stabilizing the $LiCo_xM_{1-x}O_2$ structure or by utilizing new and low cost cathode materials, such as $LiMnO_2$, $LiMPO_4$ (M = Mn, Fe). Similarly, efforts have also been made in replacing carbon anodes with high capacity tin-based materials [3]. The rate capabilities of batteries can be enhanced by reducing the particle size of electrode materials, since it is well established that the rate capabilities of Li-ion batteries are limited by solid-state diffusion of Li^+ within the electrode materials [4]. It has also been observed that the use of nanostructured cathodes can improve the intercalation behavior of polyvalent

* Corresponding author.

0378-7753/$ – see front matter © 2003 Elsevier B.V. All rights reserved.
doi:10.1016/j.jpowsour.2003.11.010

ions (e.g. Y^{3+}, Mg^{2+}), because of the shorter diffusion distances in nanoparticles [5]. Details on electrochemical properties of nanostructured cathodes with respect to polyvalent ions are beyond the scope of this paper and will not be discussed.

The primary objective of this work was to develop nanostructured electrode materials, which can either improve the energy density of batteries or enhance the rate capability of Li-based batteries. In this paper, we have shown that the full potential of V_2O_5, $LiMnO_2$, $LiFePO_4$ and $Li_4Ti_5O_{12}$ electrode materials can be realized by reducing the scale of the structure to the nanoscale dimensions. The enhancement in performance is attributed to (i) a much shorter diffusion distance for the intercalating Li-ions and (ii) the occurrence of small dimensional changes as Li-ions are cycled in and out of the nanophase intercalation compounds. In addition, the electrochemical properties are closely related to the structure and morphology of the nanoparticles.

2. Experimental

V_2O_5 nanopowders were produced using the combustion flame–chemical vapor condensation (CF–CVC) process. Details of the CF–CVC system and the process parameters, are described elsewhere [6,7]. In brief, a flat flame burner, that operates at low pressure (<66 mbar), is housed in a vacuum chamber. A cold substrate is placed between the burner and the port through which gases exit the chamber. Precursor vapors are mixed with combustibles at the rear end of the burner. Precursor molecules are pyrolyzed in the hot zone of the flame and condensed into nanoparticles as the temperature of the gas falls rapidly.

Vanadium trisopropoxide ($VO(C_3H_7)_3$), which is a liquid metalorganic precursor, was used because of its high vapor pressure (0.5 mm/60–61 °C). The precursor was heated to a temperature ranging from 70 to 135 °C at ~30 mm pressure. Vanadium precursor was pyrolyzed in a hydrogen/oxygen flame. Processing parameters, such as precursor concentration, fuel to oxygen ratio, residence time of particles in the flame and method of collection, were changed to produce VO_x nanopowders with different particle characteristics.

Nanostructured $LiMn_xM_{1-x}O_2$ and $LiFePO_4$ powders were prepared by solution methods. In case of nanostructured $LiMn_xM_{1-x}O_2$, powders were precipitated using Na_2CO_3 and $Mn(CH_3COO)_2{\cdot}4H_2O$ as the source of the main components. Cation dopants, such as Al, Co or V, were added using either inorganic salts or metal oxides. The precipitated powders were calcined at a low temperature (≤300 °C) in an oxidizing atmosphere, subsequent to which they were annealed at a temperature between 600 and 800 °C in an inert atmosphere to form the crystalline phase. Crystallized $NaMn_xM_{1-x}O_2$ powders were then lithiated by exchanging sodium ions with Li in a LiBr-alcohol solution as described by Armstrong et al. [8]. In case of $LiFePO_4$, powders were precipitated using $LiOOCCH_3{\cdot}2H_2O$, iron hydroxide and $NH_4H_2PO_4$ as the source of the main components. Precipitated powders were calcined at a low temperature, <350 °C, and annealed at a temperature between 550 and 800 °C. Powders were calcined and annealed in an inert atmosphere, if not mentioned otherwise. In a few cases, $LiFePO_4$/C composite powders were also produced by using a vapor phase process, where carbon particles were deposited on the surface of $LiFePO_4$ powders by controlling the activity of carbon in the gas phase and heating $LiFePO_4$ powders to an elevated temperature. Ultrafine $Li_4Ti_5O_{12}$ powders were produced using a wet chemical method where TiO_2 nanoparticles (primary particle ~25–30 nm), produced by the CF–CVC process and $LiNO_3$ were used as starting materials.

Electrochemical characterizations of V_2O_5, $LiMnO_2$ and $Li_4Ti_5O_{12}$ electrodes was performed in a standard coin cell configuration. Electrodes were fabricated by mixing ~65 wt.% oxide powder, 10 wt.% polyvinylidene fluoride based copolymer binder, 7 wt.% conductive black and 18 wt.% dibutyl phthalate plasticizer in acetone solvent for 1 h. The slurry was cast on glass and dried in ambient. Disks were punched out of the resulting plastic tape; these disks were placed in ether to extract the plasticizer. Li metal on Ni foil was used as anode; the electrolyte was 1 M $LiPF_6$, dissolved in ethylene carbonate and dimethyl carbonate in a 2:1 volume ratio. All cells used Whatman GF/D glass fiber separators. Electrochemical characterization was performed on either MacPile (BioLogic) or Moli (Moli Energy) galvanostat/potentiostat. Li/$LiMnO_2$ cells tested at current densities of 2.5 and 52.5 mA/g were fabricated by mixing oxide powder with carbon powder and PTFE binder in a weight ratio of 60:30:10 in cyclohexane. After evaporating cyclohexane in vacuum, the mixture was rolled, punched and pressed into diameter pellets with a thickness of 150–200 μm. The pellets were then dried at 80 °C in vacuum for 24 h and tested in laboratory glass cells. Li foils were used as the counter and reference electrodes; the electrolyte was of 1 M $LiClO_4$ in DME. A Solartron battery tester was used for charge/discharge tests.

In case of $LiFePO_4$, coin cells (CR2032) were fabricated with $LiFePO_4$ cathodes (circular electrodes of 9 mm diameter and ~8 mg mass) containing 20 wt.% fine carbon (Denka Black) and 5 wt.% polytetrafluoroethylene (PTFE) binder (Teflon 6-J, DuPont-Mitsui Fluorochemical Co. Ltd), metallic lithium foil anodes, polyethylene separator (Tohnen Setera, Japan) and $LiPF_6$ in ethylene carbonate (EC)/diethyl carbonate (DEC) electrolyte. The coin cells were subjected to charge/discharge cycling between 2 and 4.2 V versus lithium with various current densities of 0.05 (*C*/16 rate) and 0.1 (*C*/8 rate) at room temperature, assuming a reversible capacity of 90 mAh/g at *C*/8 rate. In general, $LiFePO_4$ samples were tested at a current density of 0.1 mA/cm^2, if not mentioned otherwise.

3. Results and discussion

3.1. V_2O_5 cathodes

In the CF–CVC process, nanoparticles are formed by condensation of pyrolyzed clusters as the temperature of gas falls off sharply. Hot nanoparticles are quenched rapidly with a cooling rate as high as $\sim 10^7$ °C/min. Consequently, it is possible to produce kinetically stabilized amorphous or metastable structures of 'discrete' nanoparticles by changing processing parameters. Nano-V_2O_5 properties, such as crystal structure, primary particle size and morphology, were varied by changing the processing conditions in the CF–CVC process. One set of flame conditions yielded V_2O_5 nanopowders with a metastable structure. A powder X-ray diffraction pattern on the metastable powder, Fig. 1, shows two large broad peaks, which are typical of amorphous or amorphous-like regions. In addition to broad peaks, there are two small sharp peaks that correspond to V_2O_5. TEM observation shows that the nanopowder consists of "discrete" nanoparticles in a size-range, 30–50 nm, Fig. 2. Additionally, high resolution TEM micrograph also shows the crystalline regions within the discrete nanoparticles. Combining this TEM observation with XRD data, it is clear that nanoparticles have both both crystalline and amorphous regions. This kind of a metastable structure is stabilized because of the rapid kinetics of the CF–CVC process [9].

Cathodes made of V_2O_5 powders were tested over two voltage regimes: 4.2–2.5 and 4.2–1.5 V. The discharge–charge curves (4.2–1.5 V) of nano-V_2O_5 and coarse (crystalline) V_2O_5 powders are shown in Fig. 3. Nano-V_2O_5 has a smooth voltage profile, on the other hand, standard crystalline V_2O_5 has a discontinuous voltage profile, a feature that is undesirable for practical rechargeable Li-batteries. Similar behavior was also observed for the voltage profile in the range of 4.2–2.5 V [9].

Specific capacity of cathodes using nanoscale and standard coarse V_2O_5 powders for discharge–charge voltage ranges of 4.2–2.5 and 4.2–1.5 V are shown in Fig. 4. In case of a discharge–charge voltage of 4.2–2.5 V, nano-V_2O_5 had a capacity of 170 mAh/g after 14 discharge–charge cycles. However, the capacity of coarse V_2O_5 cathodes was only 130 mAh/g for the same number of cycles, i.e. nanopowders have a retention capacity almost 30% higher than that of commercial V_2O_5 powders. In case of lower discharge voltage (1.5 V), the specific retention capacity of nano-V_2O_5 is 50% greater than that of standard crystalline V_2O_5 powders for same number of cycles. Capacities of nanopowder and commercial V_2O_5 are 310 and 190 mAh/g, respectively, after eight cycles. Furthermore, the irreversible capacity loss in the first discharge cycle is much lower for nano-V_2O_5 as compared to that of commercial V_2O_5. The irreversible capacity loss for the lower discharge voltage

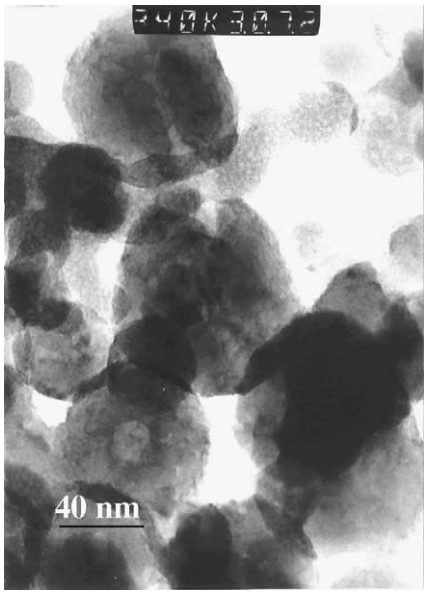

Fig. 2. High resolution TEM micrograph [3].

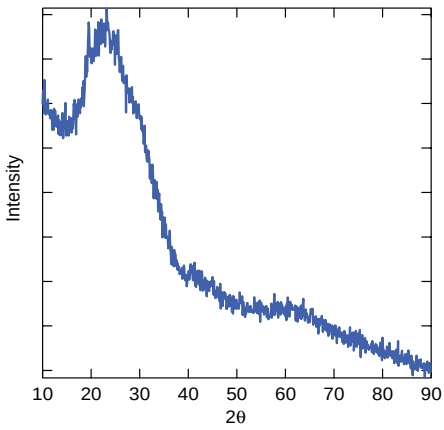

Fig. 1. Powder X-ray diffraction data of a V_2O_5 nanopowder, which is synthesized by the CF–CVC process.

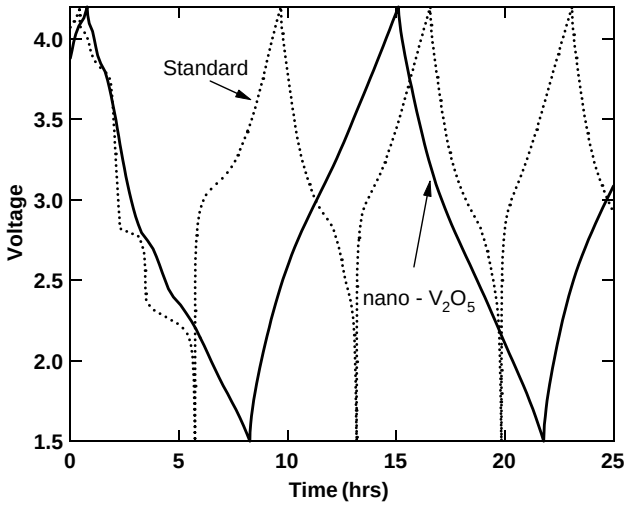

Fig. 3. Voltage curves (4.2–1.5 V) as a function of discharge/charge time for nanoscale (solid) and standard coarse (dotted) V_2O_5 powders.

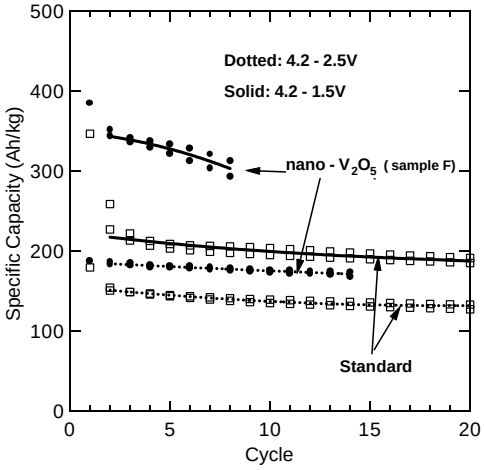

Fig. 4. Capacity of nanoscale and standard V_2O_5 powders as a function of the total number of cycles for high (4.2–2.5 V) and low (4.2–1.5 V) discharge voltages.

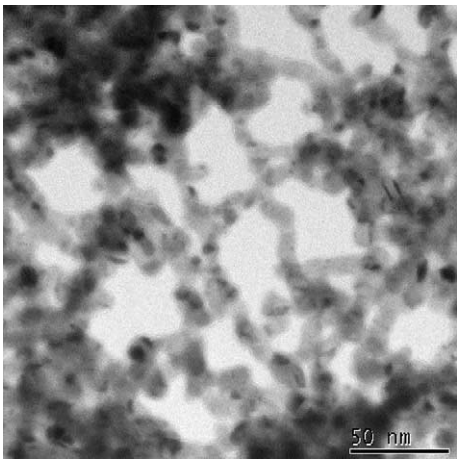

Fig. 5. A TEM micrograph of a nano-$LiFePO_4$ powder.

(4.2–1.5 V) of nano-V_2O_5 and commercial V_2O_5 cathodes is 9 and 26%, respectively. In case of the higher discharge voltage (4.2–2.5 V), the irreversible capacity loss of commercial V_2O_5 is 16%; on the other hand, it is negligible for nano-V_2O_5 cathodes. The unique structure of nanoparticles could be responsible for a lower irreversible capacity loss particularly at a discharge voltage of 4.5–1.5 V. Typically, for this discharge voltage range, macrocrystalline V_2O_5 transforms to ω-phase by a destructive transformation mechanism. As a result, macrocrystalline V_2O_5 exhibits substantial irreversible capacity loss. It is possible that metastable nanoparticles do not transform to the ω-phase; thus, do not experience a high irreversible capacity loss.

In addition to electrochemical properties, packing density of cathode is also important for higher volumetric energy density. It is known that the bulk density of aerogels is low, ∼0.1–0.2 g cm^3. As a result, these materials can not be packed efficiently in polymer tapes. In order to determine the packing density of our nanopowders, two tapes were fabricated: one using nano-V_2O_5, and the other using coarse powders (1–10 μm). Powders were mixed with carbon black, PVDF and a plasticizer and cast as tape, which was laminated and pressed together. Subsequently, the plasticizer was removed by evaporation. We achieved 70 wt.% loading with V_2O_5 nanopowders. In conventional electrodes fabricated by battery manufacturers, 80 wt.% loading is considered standard for coarse powders. The bulk density of tape containing nanoparticles was 1.6 g/cm^3, which is 93% of bulk density of the tape containing coarse powders. The difference in density is due to the residual porosity, which can be eliminated by optimizing the process.

TEM and XRD results on nanopowders suggest that it is possible to use the CF–CVC process to produce nanoparticles with novel structures. By controlling the temperature of the hot zone and the residence time of nanoparticles in the gas phase, it is possible to tune the extent of crystallization while maintaining the discrete nanoparticulate morphology. Furthermore, results suggest that "discrete" nanoparticles with a metastable structure improve the electrochemical performance of V_2O_5 cathodes in a Li-cell. The correlation between structure, composition and morphology of particles with the corresponding electrochemical properties in a rechargeable Li-ion battery is a subject of future research.

3.2. *$LiFePO_4$ cathodes*

We produced nano-$LiFePO_4$ powders with a crystallite size in the range of 5–50 nm, Fig. 5. Although cathodes made of these nanostructured powders exhibited structural stability and virtually no capacity loss during electrochemical cycling in Li-test cells, the specific capacity was only ∼90 mAh/g. It is well known that the electronic conductivity of $LiFePO_4$ is quite poor. Therefore, we synthesized $LiFePO_4$/C composites to enhance the electronic conductivity of $LiFePO_4$ cathodes. Cathodes made of $LiFePO_4$/C powders exhibited relatively high capacity, ∼145 mAh/g,[1] Fig. 6. The total amount of carbon in the powder was ∼37 wt.%. These results demonstrate that the poor electronic conductivity of $LiFePO_4$ can be overcome so that they can be utilized in commercial Li-ion batteries. However, still significant effort has to be made to reduce the amount of carbon in the composite and to further improve the rate capabilities of $LiFePO_4$/C cathodes.

3.3. *Layered $LiMnO_2$ cathodes*

Layered $LiMnO_2$ suffers from structural instability during electrochemical cycling and as a result, exhibits significant capacity fade [10]. Furthermore, macrocrystalline materials have poor rate capabilities. Substantial efforts have been made to stabilize the layered structure [8,11–14]

[1] Capacity calculations do not include the carbon content in the composite powder.

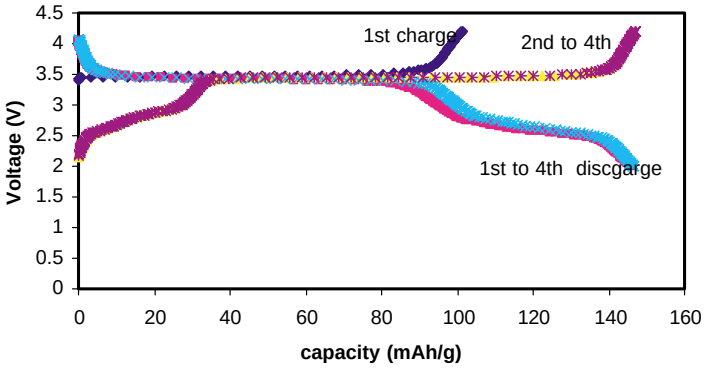

Fig. 6. Voltage versus capacity curve for a positive electrode made of nano-$LiFePO_4$/C composite powder in a Li-test cell. It is to be noted that in capacity data calculations, the amount of carbon (37 wt.%) in the composite was excluded.

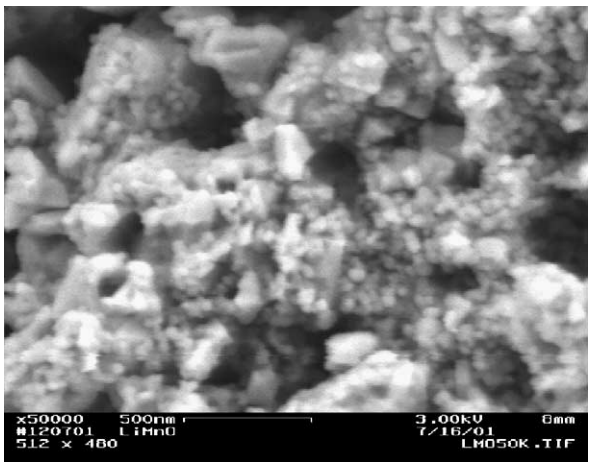

Fig. 7. A FESEM micrograph of a nano-$LiMn_xM_{1-x}O_2$ powder.

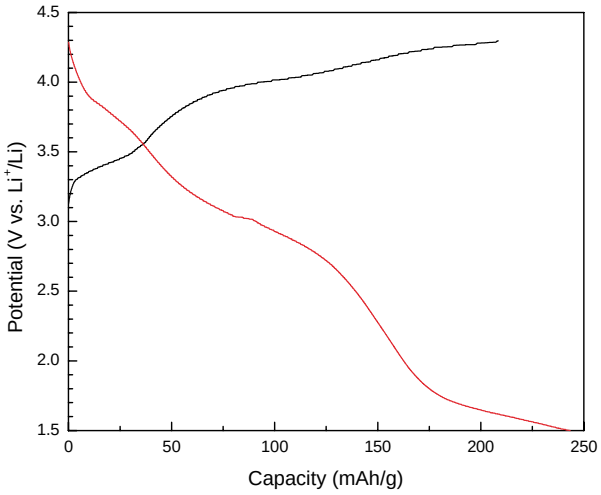

Fig. 9. A charge/discharge curve of a nano-$LiMn_xM_{1-x}O_2$ cathodes in a Li-test cell at a current density of 2.7 mA/g.

by substituting Mn with cation dopants, such as Al and Co. The focus of our work has been to develop layered $LiMn_xM_{1-x}O_2$ cathode materials that have nanoscale features. To the best of our knowledge, this is the first time that a nano-$LiMn_xM_{1-x}O_2$ compound with a layered structure has ever been synthesized. A FESEM micrograph (Fig. 7) of $LiMn_xM_{1-x}O_2$ powders shows the nanostructured nature of the particles. X-ray data, Fig. 8, exhibit broad peaks of a layered, monoclinic $LiMnO_2$ compound.

Fig. 9 shows the charge/discharge curves of the sample under low current density of 2.7 mA/g at room temperature. Nano-$LiMn_xM_{1-x}O_2$ cathodes possessed an open circuit voltage of 3.2 V vs Li^+/Li. First charge capacity of nano-$LiMn_xM_{1-x}O_2$ is 210 mAh/g, while nano-$LiMn_xM_{1-x}O_2$ cathodes can be discharged up to a capacity of 245 mAh/g in a Li-cell for a voltage range of 4.2–1.5 V. Furthermore, nano-$LiMn_xM_{1-x}O_2$ cathodes exhibited a small intercalation capacity, ~35 mAh/g, when they were discharged initially. Data suggest that as

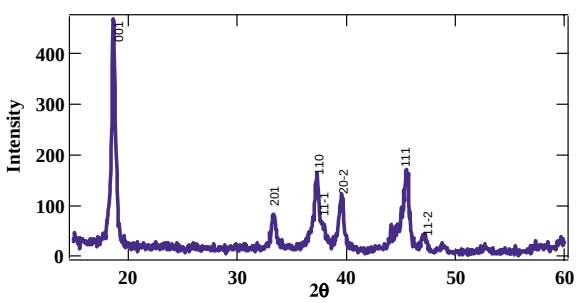

Fig. 8. X-ray diffraction pattern of a nano-$LiMn_xM_{1-x}O_2$ powder with a layered structure.

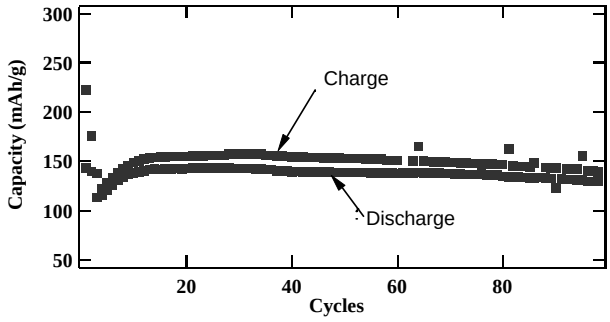

Fig. 10. Retention capacity of nano-$LiMn_xM_{1-x}O_2$ cathodes cycled between 4.2 and 2.0 V at a current density of 22.5 mA/g.

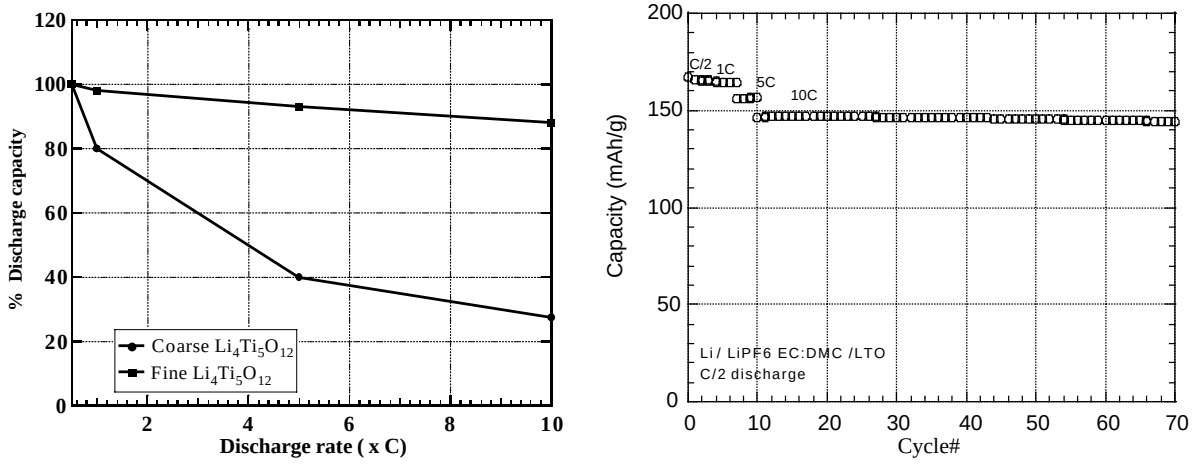

Fig. 11. (a) Performance of test cells ($Li/Li_4Ti_5O_{12}$) at different discharge rates for both fine and coarse $Li_4Ti_5O_{12}$ powders and (b) cycling performance of ultrafine $Li_4Ti_5O_{12}$ powders at different discharge rates.

synthesized nano-$LiMn_xM_{1-x}O_2$ powders could be deficient in Li. First discharge/charge curves of nano-$LiMn_xM_{1-x}O_2$ showed two voltage plateaus at about 3.4 and 4.0 V, though these voltage plateaus were not as prominent as they would be in case of macrocrystalline layered $LiMnO_2$ cathodes [7]. On increasing the discharge current density from 2.7 to 53.7 mA/g, the discharge capacity decreased from 245 to 150 mAh/g. On discharging and charging at a current density of 22.5 mA/g,[2] nanostructured $LiMn_xM_{1-x}O_2$ did not show significant capacity fading on cycling, Fig. 10. Presently, we are optimizing composition and structure of nano-$LiMn_xM_{1-x}O_2$ particles for improving their rate capabilities.

3.4. $Li_4Ti_5O_{12}$ anodes

Rechargeable energy storage devices are being used in increasing number in several consumer applications, such as hybrid electric vehicles, wireless communication devices, uninterrupted power sources and power tools. A lightweight, compact and high-power density energy storage device with excellent charging rate capability and cyclability (thousands of cycles) is desired for the above mentioned applications. For example, energy storage devices for hybrid electric vehicles (HEVs) should possess high power density (~2000 W/kg) and fast charge rate (>10 C) capabilities, along with reasonable energy density and excellent cycle life, since the hybrid propulsion system in next generation vehicles requires to recapture the vehicle kinetic energy through regenerative braking. Lead-acid and Ni–Cd batteries, which are presently being used for these applications, suffer from either low cycling life, poor charge retention, limited charging rate capabilities, or environmental issues. Consequently, high rate energy storage technologies, such as high power Li-ion batteries and asymmetric hybrid batteries [15] (which charges and discharges in a few minutes like a supercapacitor and also exhibits an order of magnitude higher energy density than a supercapacitor), are being considered. $Li_4Ti_5O_{12}$ is a suitable anode material for both high power Li-ion batteries and asymmetric hybrid batteries, because of its excellent structural stability (no dimensional changes as Li-ions go in and out of the material) and no risk of Li-plating during the fast charge rate as the reduction potential of $Li_4Ti_5O_{12}$ is 1.5 V versus Li^+/Li.

$Li/Li_4Ti_5O_{12}$ test cells were fabricated using both ultrafine and coarse $Li_4Ti_5O_{12}$ powders. Cells made with ultrafine $Li_4Ti_5O_{12}$ as anodes discharged to 90% of their initial capacity at a rate of 10 C, while those with anodes consisting of coarse $Li_4Ti_5O_{12}$ discharged only to 30% at the same discharge rate, Fig. 11(a). Presumably, smaller particles have shorter diffusion distances for intercalated Li-ions, resulting in a higher charge rate for intercalated anodes. In addition to excellent high discharge rate capability, the cycling life of ultrafine $Li_4Ti_5O_{12}$ was excellent at high discharge rates. The total capacity fade at a discharge rate of 10 C was <10% after 70 cycles, Fig. 11(b).

[2] For the initial two discharge and charge cycles, the current density was 7.5 mA/g.

Acknowledgements

We would like to acknowledge US Department of Energy (Contract # DE-FG02-01FR83219), National Aeronautics and Space Administration (Contract # NAS9-02023) and Missile Defense Agency (Contract # DASG60-01-C-0086) for funding this work.

References

[1] D.R. Sadoway, A.M. Mayes, MRS Bull. 27 (8) (2002) 590.
[2] J.M. Tarascon, M. Armand, Nature 414 (2001) 359.
[3] Y. Idota, T. Kubota, A. Matsufuji, Y. Maekawa, T. Miyasaka, Science 276 (1997) 1395.

[4] C.R. Sides, N. Li, C.J. Patrissi, B. Scrosati, C.R. Martin, MRS Bull. 27 (8) (2002) 604.
[5] G.G. Amatucci, F. Badway, A. Singhal, B. Beaudoin, G. Skandan, T. Bowmer, I. Plitz, N. Periera, T. Chapman, R. Jawoski, J. Electrochem. Soc. 148 (8) (2001) A940.
[6] G. Skandan, Y.-J. Chen, N. Glumac, B.H. Kear, Nanostruct. Mater. 11 (1999) 149.
[7] A. Singhal, G. Skandan, A. Wang, N. Glumac, B.H. Kear, R.D. Hunt, Nanostruct. Mater. 11 (1999) 545.
[8] A.R. Armstrong, A.D. Robertson, P.G. Bruce, Electrochim. Acta 45 (1999) 285–294;
A.R. Armstrong, R. Gitzendanner, A.D. Robertson, P.G. Bruce, Chem. Commun. 1833 (1998).
[9] A. Singhal, G. Skandan, G. Amatucci, N. Pereira, Nanostructured electrodes for rechargeable Li Batteries, in: Proceedings of the Volume of Electrochemical Society—Workshop on Interfaces, Phenomena and Nanostructures in Lithium Batteries, Argonne, 11–13 December 2000.
[10] M. Thackeray, Prog. Solid State Chem. 25 (1997) 1.
[11] Y. Jang, B. Huang, Y.-M. Chiang, D.R. Sadoway, Electrochem. Solid State Lett. 1 (1998) 13.
[12] Y.M. Chaing, D.R. Sadoway, Y. Jang II, B. Huang, H. Wang, Electrochem. Solid State Lett. 2 (1999) 107.
[13] H. Nakano, Y. Ukyo, T. Honma, US patent 6,306,542 (2001).
[14] J.M. Paulsen, C.L. Thomas, J.R. Dahn, J. Electrochem. Soc. 146 (1999) 3560.
[15] G.G. Amatucci, F. Badway, A.D. Pasquier, T. Zheng, J. Electrochem. Soc. 148 (8) (2001) A930–A939.